

## PHYSICAL PROPERTIES OF THE AXP 4U 0142+61 FROM X-RAY SPECTRAL ANALYSIS

TOLGA GÜVER,<sup>1</sup> FERYAL ÖZEL,<sup>1</sup> AND ERSİN GÖĞÜŞ<sup>2</sup>  
*Received 2007 May 10; accepted 2007 November 6*

### ABSTRACT

We analyze archival *Chandra* and *XMM-Newton* data of 4U 0142+61 within the context of the surface thermal emission and magnetospheric scattering model. We show that the 4U 0142+61 spectrum can be fit very well with this physical model that contains only four parameters. The system parameters can be tightly constrained from the fits, yielding a surface magnetic field strength of  $B = (4.75 \pm 0.02) \times 10^{14}$  G, a surface temperature of  $kT = 0.309 \pm 0.001$  keV, and a scattering optical depth of a few in the magnetosphere. These values do not vary between observations due to the stability of the source within the window of the observations. The detailed fits yield  $\chi^2$  values that are statistically much better than the traditionally employed blackbody+power-law and two blackbody fits. The spectroscopically measured surface magnetic field strength is higher than, but within, the theoretical uncertainties of the value inferred from the dipole spin-down formula.

*Subject headings:* pulsars: individual (4U 0142+61) — stars: neutron — X-rays: stars

*Online material:* color figures

### 1. INTRODUCTION

Anomalous X-ray pulsars (AXPs) and soft gamma repeaters (SGRs) are thought to be the observational manifestations of a class of ultramagnetic ( $B \gtrsim 10^{14}$  G) neutron stars, also called magnetars (see Woods & Thompson 2006 and Kaspi 2007 for a detailed review on AXPs and SGRs). The strong magnetic fields are believed to power the X-ray emission of these neutron stars and give rise to high spin-down rates ( $\dot{P} \sim 10^{-11}$  s s<sup>-1</sup>; Thompson & Duncan 1996). Furthermore, the large reservoir of magnetic energy associated with such fields leads to intense, super-Eddington ( $L \gtrsim L_{\text{Edd}}$ ), random bursts of X-rays or soft gamma rays. Indeed, observations of such powerful bursts that typically last a fraction of a second and have been detected from all four known SGRs and at least five out of the eight known AXPs lend strong, albeit indirect, support for their identification as magnetars (Gavriil & Kaspi 2002; Kaspi et al. 2003; Woods et al. 2005).

AXPs and SGRs are all observed as point X-ray sources with luminosities of  $10^{33}$ – $10^{36}$  erg s<sup>-1</sup>. Their X-ray spectra, in the 0.5–10.0 keV photon energy range, have so far been described by empirical functions such as a blackbody ( $kT \sim 0.3$ – $0.6$  keV) plus a power law (with photon index  $\Gamma \sim 2.5$ – $4$ ) and, less frequently, by a sum of two blackbody functions (see, e.g., Gotthelf & Halpern 2007; Kaspi 2007). Within the magnetar model, the blackbody component is attributed to the emission from the neutron star surface that is heated by the decay of the strong magnetic field (Thompson & Duncan 1996). The power-law component, on the other hand, is thought to be magnetospheric in origin and is widely used to obtain a better representation of the X-ray spectra.

We have recently developed a physical model of emission from a magnetar that takes into account processes in its atmosphere, as well as in its magnetosphere. The surface thermal emission and magnetospheric scattering (STEMS) model is based on the radiative equilibrium atmosphere calculations presented in Özel (2003) but also includes the effects of magnetospheric scattering of the surface radiation as discussed in Thompson et al. (2002),

Lyutikov & Gavriil (2006), and Güver et al. (2007). Our models predict strong deviations from a Planckian spectrum, with a hard excess that depends on the surface temperature, as well as the magnetic field strength (Özel & Güver 2007), and weak absorption lines due to the proton cyclotron resonance. Both the atmospheric processes and the magnetospheric scattering play a role in forming these spectral features and especially in reducing the equivalent widths of the cyclotron lines.

With the first successful application of this model (Güver et al. 2007), we fit the spectrum of the AXP XTE J1810–197, a transient source whose flux showed more than 2 orders of magnitude variation during the three years it has been monitored (Gotthelf & Halpern 2007). In contrast, 4U 0142+61 is the brightest and historically a stable AXP. Following its detection with *Uhuru*, an *EXOSAT* campaign revealed its neutron star nature by the discovery of its 8.7 s periodicity (Israel et al. 1994). Multiple X-ray observations of the source showed a long epoch of nearly constant flux levels, as well as a relatively hard X-ray spectrum (White et al. 1996; Juett et al. 2002; Patel et al. 2003; Göhler et al. 2005). Recently, the source exhibited SGR-like bursts (Kaspi et al. 2006; Dib et al. 2006; Gavriil et al. 2007) for the first time.

4U 0142+61 has also been detected in hard X-rays with *INTEGRAL* (Kuiper et al. 2006; den Hartog et al. 2004, 2007). The hard X-ray spectral component in the 20–230 keV energy range is well described by a power-law model of index 0.79, and the corresponding flux is  $1.7 \times 10^{-10}$  erg cm<sup>-2</sup> s<sup>-1</sup> (den Hartog et al. 2007), which exceeds by a factor of  $\sim 2$  the unabsorbed 2–10 keV flux. It is noteworthy that the extrapolation of the power-law component toward lower photon energies yields flux levels that contribute significantly to the soft X-ray flux at the 7–10 keV range. Furthermore, the fact that the hard X-ray component is pulsed and is in phase with soft X-rays (Kuiper et al. 2006) points to a connection between the hard and soft components. Rea et al. (2007) attempted to model the combined soft and hard X-ray spectrum with a variety of empirical functions and a model that treats resonant scattering in the magnetosphere and showed that some of these empirical models were feasible.

Durant & van Kerkwijk (2006a) measured the Galactic column density to some of the AXPs, using the individual absorption edges of the elements O, Fe, Ne, Mg, and Si. They found the column density to 4U 0142+61 to be  $(0.64 \pm 0.07) \times 10^{22}$  cm<sup>-2</sup>,

<sup>1</sup> Department of Physics, University of Arizona, 1118 East 4th Street, Tucson, AZ 85721.

<sup>2</sup> Faculty of Engineering Natural Sciences, Sabancı University, 34956, Orhanli-Tuzla, Istanbul, Turkey.

TABLE 1  
OBSERVATIONS USED FOR THIS STUDY

Satellite	Detector	Mode	Exposure Time (ks)	Observation ID	Observation Date
<i>Chandra</i> .....	ACIS-S	CC	5.94	724	2001 May 21
<i>XMM-Newton</i> .....	EPIC-PN	Small window	1.9	0112780301	2002 Feb 13
			4.0	0112781101	2003 Jan 24
		Fast timing	35.78	0206670101	2004 Mar 01
			21.1	0206670201	2004 Jul 25

a factor of 1.4 lower than the value inferred from the blackbody plus power-law fits. Using the red clump stars (core-helium-burning giants) in the direction of the source to measure the variation of the reddening with distance and extinction, Durant & van Kerkwijk (2006b) also determined the distance of the source as 3.6 kpc.

In this paper, we analyze archival *Chandra* and *XMM-Newton* data of 4U 0142+61 within the context of the STEMS model and obtain physical system parameters by performing detailed fits to the soft X-ray spectra of this source. In § 2, we describe our physical model. In § 3, we present the data and the fit results. We conclude in § 4 with a discussion of our results and their implications.

## 2. THE SURFACE THERMAL EMISSION AND MAGNETOSPHERIC SCATTERING MODEL

The spectrum of a magnetar is molded by its atmosphere and its magnetosphere. In the ionized, highly magnetic neutron star atmospheres, polarization mode-dependent transport of radiation that includes absorption, emission, and scattering processes determines the continuum spectrum (see, e.g., Özel 2001, 2003; Lai & Ho 2003). Furthermore, the interaction of the photons with the protons in the plasma gives rise to an absorption feature at the proton cyclotron energy

$$E_p = 6.3 \left( \frac{B}{10^{15} \text{ G}} \right) \text{ keV}. \quad (1)$$

This absorption feature is weakened by the vacuum polarization resonance, which also leads to an enhanced conversion between photons of different polarization modes as they propagate through the atmosphere.

In the magnetospheres, currents supporting the ultrastrong magnetic fields can lead to enhanced charge densities (Thompson et al. 2002), which can reprocess the surface radiation through resonant cyclotron scattering (Lyutikov & Gavriil 2006; Güver et al. 2006). We calculate this effect using the Green's function approach described in Lyutikov & Gavriil (2006) assuming that the magnetosphere is spherically symmetric and the field strength follows a  $1/r^3$  dependence.

We have developed a spectral model that includes these relevant mechanisms that take place on the magnetar surface and its magnetosphere and depends only on four physical parameters. The first two parameters, the surface magnetic field strength  $B$  and temperature  $T$ , describe the conditions found on the neutron star surface. The third parameter denotes the average energy of the charges  $\beta = v_e/c$  in the magnetosphere, while the last parameter is related to the density  $N_e$  of such charges and indicates the optical depth to resonant scattering by

$$\tau = \sigma \int N_e dz. \quad (2)$$

Here  $\sigma$  is the cross section for resonant cyclotron scattering. We also assume a fixed value for the gravitational acceleration on the neutron star surface of  $1.9 \times 10^{14} \text{ cm s}^{-2}$ , obtained for reasonable values of the neutron star mass and radius.

We calculated model X-ray spectra (in the 0.05–9.8 keV range) by varying model parameters in suitable ranges that are in line with the physical processes that we incorporated into the models: surface temperature  $T = 0.1$ –0.6 keV, magnetic field  $B = 5 \times 10^{13}$  to  $3 \times 10^{15}$  G, electron velocity  $\beta = 0.1$ –0.5, and optical depth in the magnetosphere  $\tau = 1$ –10. From the set of calculated spectra, we created a table model that we use within the X-ray

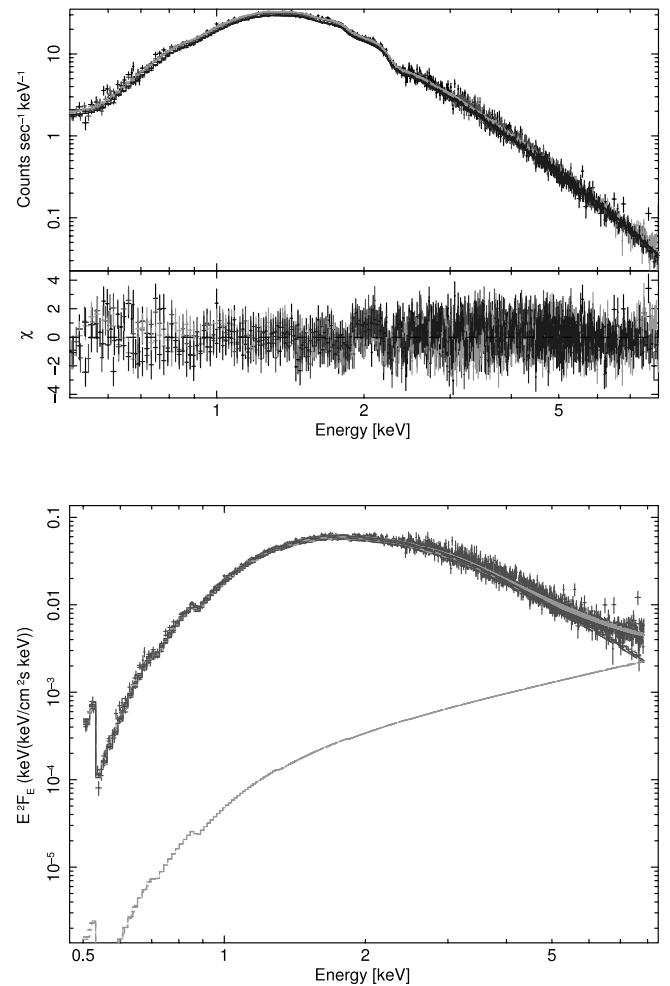


FIG. 1.— Simultaneous fit of the surface thermal emission and magnetospheric scattering model to the four data sets of the X-ray spectra of 4U 0142+61 given in Table 1. In the lower panel, the  $E^2 F_E$  spectra show the effects of the extrapolated hard X-ray component on the soft X-ray spectra. [See the electronic edition of the Journal for a color version of this figure.]

TABLE 2  
RESULTS OF THE SURFACE THERMAL EMISSION AND MAGNETOSPHERIC SCATTERING MODEL

Observation Date	$N_{\text{H}}$ ( $10^{22} \text{ cm}^{-2}$ )	Magnification Field ( $10^{14} \text{ G}$ )	Temperature (keV)	$\beta$ (counts)	$\tau$	Flux <sup>a</sup>	$\chi^2_{\nu}$ (dof)
2000 May 21.....	$0.57 \pm 0.02$	$3.96 \pm 0.31$	$0.307 \pm 0.006$	$0.46 \pm 0.02$	$5.44 \pm 0.52$	$1.92 \pm 0.20$	1.174 (283)
2002 Feb 13.....	$0.54 \pm 0.02$	$4.66 \pm 0.56$	$0.31 \pm 0.01$	$0.42 \pm 0.05$	$3.68 \pm 0.59$	$2.07 \pm 0.54$	1.027 (310)
2003 Jan 24.....	$0.55 \pm 0.02$	$5.16 \pm 0.42$	$0.31 \pm 0.01$	$0.45 \pm 0.03$	$3.16 \pm 0.33$	$2.10 \pm 0.23$	0.999 (345)
2004 Mar 1.....	$0.57 \pm 0.01$	$4.60 \pm 0.07$	$0.310 \pm 0.002$	$0.40 \pm 0.01$	$3.55 \pm 0.14$	$2.04 \pm 0.06$	0.974 (402)
2004 Jul 25.....	$0.58 \pm 0.01$	$4.67 \pm 0.16$	$0.305 \pm 0.002$	$0.43 \pm 0.01$	$3.54 \pm 0.14$	$1.98 \pm 0.07$	0.931 (462)

NOTE.—All the errors are given with 90% confidence.

<sup>a</sup> Unabsorbed 0.5–8.0 keV flux in units of  $10^{-10} \text{ erg cm}^{-2} \text{ s}^{-1}$ .

spectral analysis package XSPEC (Arnaud 1996) to model the X-ray spectra of 4U 0142+61.

### 3. OBSERVATIONS AND DATA ANALYSIS

In Table 1, we present the list of the archival pointed X-ray observations of 4U 0142+61 that we analyzed in this study. *Chandra* observations were calibrated using CIAO<sup>3</sup> version 3.4 and CALDB 3.3.0.1. For the *XMM-Newton* observations we used the Science Analysis Software (SAS) version 7.0.0 and the latest available calibration files. The *XMM-Newton* observation in 2002 was excluded from earlier studies (Göhler et al. 2005) because it was partially affected by the high-energy particle background. We were able to eliminate the segments with a high background, and were able to utilize an effective exposure of 1.9 ks out of the 3.4 ks. We used only EPIC-PN data of each *XMM-Newton* observation.

For the small window mode *XMM-Newton* observations, we extracted source spectra from a circle centered on the source with a radius of  $32''$  and the background from a source-free region with a radius of  $50''$ . We extracted the source region from the CC mode *Chandra* observation using a rectangular region centered on the source with sizes  $8'' \times 2''$ , and used as the background region from this data set a source-free region with similar sizes. For the *XMM-Newton* observations in the fast-timing mode, we extracted the source spectrum from a rectangular region of 9.5 pixels centered on the source, and used a background spectrum with similar sizes from a source-free region on the CCD. To create the response and ancillary response files, we used the `mkacisrmf`, `mkarf`, and `epproc` tasks for *Chandra* and *XMM-Newton* data sets, respectively. We rebinned *XMM-Newton* spectra such that each energy bin contains at least 50 counts without oversampling the energy resolution of the instrument. To account for the calibration uncertainties we have also included a 2% systematic error in all fits.

The spectral analysis was performed using XSPEC 11.3.2.t (Arnaud 1996). We assumed a fiducial gravitational redshift correction of 0.2, which corresponds to a neutron star with mass  $1.4 M_{\odot}$  and  $R = 13.8 \text{ km}$ . We calculate the fluxes for the 0.5–8.0 keV energy range and quote errors for 90% confidence level. For the calculation of Galactic column density, we have used Anders & Grevesse (1989) solar abundances.

#### 3.1. Results of Spectral Modeling

In our analysis, we take into account the contribution of the hard X-ray emission to the 0.5–8.0 keV spectra by adding a power-law component with frozen parameters given by den Hartog et al. (2007). In doing so, we assume that this hard power-law com-

ponent extends down to the soft X-ray band without a break and thus has a nonnegligible contribution to the overall flux above 6.5 keV. In addition, we take into account the independent results of Durant & van Kerkwijk (2006a) to evaluate the performance of the models at low energies.

The spectral properties of 4U 0142+61 do not vary significantly throughout the four years spanned by the observations. We, therefore, first fit all *XMM-Newton* EPIC-PN spectra simultaneously in order to better constrain model parameters. Note that we excluded *Chandra* ACIS-S observation from the simultaneous fit to avoid any systematic uncertainties due to different calibration schemes. We obtained an excellent fit to data,  $\chi^2_{\nu} = 0.949$  for 1534 degrees of freedom (dof), with flat residuals. The data, best-fit model, and the residuals are shown in Figure 1.

The fit provides tight constraint on the model parameters: the surface temperature,  $kT = 0.309 \pm 0.001 \text{ keV}$ , the surface magnetic field strength  $B = (4.75 \pm 0.02) \times 10^{14} \text{ G}$ , the optical depth to scattering in the magnetosphere,  $\tau = 3.57 \pm 0.03$ , and a thermal particle velocity in the magnetosphere  $\beta = 0.417 \pm 0.002$ .

For the hydrogen column density, we obtain  $N_{\text{H}} = (0.566 \pm 0.002) \times 10^{22} \text{ cm}^{-2}$ , which is in good agreement with the value [of  $N_{\text{H}} = (0.64 \pm 0.07) \times 10^{22} \text{ cm}^{-2}$ ] found by Durant & van Kerkwijk (2006a). If we, instead, demand an exact correspondence with the latter value by freezing the column density at  $0.64 \times 10^{22} \text{ cm}^{-2}$ , we obtain a somewhat poorer fit ( $\chi^2_{\nu} = 1.361$  for 1535 dof).

We also fit each spectrum individually with the STEMS model. We find that our model produces excellent fits to all individual spectra. In Table 2, we present the results of the individual spectral fits. The obtained values of the parameters are consistent with each other within  $1 \sigma$ , as well as with the results of the simultaneous fit.

For comparison, we have also used the empirical blackbody plus power-law model to fit all *XMM-Newton* data simultaneously (still allowing for a contribution from the extension of the hard X-ray power-law component). The result is acceptable within the context of X-ray spectroscopy ( $\chi^2_{\nu}$  of 1.349 for 1532 dof); however, the residuals, especially at  $\lesssim 2 \text{ keV}$ , are not flat (see Fig. 2, *upper panel*) and do not capture the characteristics of the spectrum. Correspondingly, the  $\chi^2_{\nu}$  value is worse than that we obtain for our STEMS fits even though the STEMS model has two fewer parameters than the blackbody plus power-law model.<sup>4</sup> For the blackbody plus power-law fit, we obtain model parameters of

<sup>4</sup> Note that to describe each data set the blackbody plus power-law model requires one fewer parameters than the STEMS model. However, we allow the normalizations of the blackbody and the power-law components to vary independently for the description of each data set, resulting in a total of 11 free parameters in the simultaneous fit to four data sets. On the other hand, the STEMS model has one normalization per data set, which yields a total number of nine free parameters for the four data sets.

<sup>3</sup> See <http://xc.harvard.edu>.

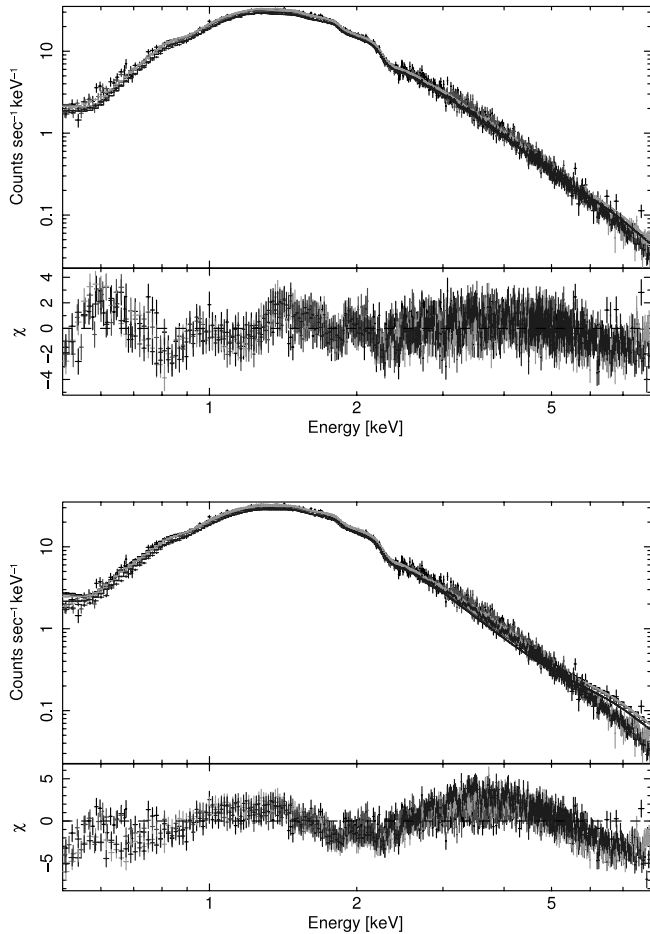


FIG. 2.—Simultaneous blackbody plus power-law model fit to the X-ray spectra of 4U 0142+61. The upper panel shows the fit when the hydrogen column density  $N_{\text{H}}$  is allowed to vary, while the lower panel corresponds to  $N_{\text{H}}$  frozen at  $0.64 \times 10^{22} \text{ cm}^{-2}$ , the value measured independently by Durant & van Kerkwijk (2006a). [See the electronic edition of the *Journal* for a color version of this figure.]

$N_{\text{H}} = (1.001 \pm 0.002) \times 10^{22} \text{ cm}^{-2}$ , a blackbody temperature of  $0.431 \pm 0.001 \text{ keV}$ , and a photon index of  $3.94 \pm 0.01$  (see Fig. 2, upper panel). Note that the column density is 1.6 times ( $92 \sigma$ ) higher than the value reported by Durant & van Kerkwijk (2006a) through a different and spectral model-independent analysis. Because it shows this large disagreement, we also tried a fit where the column density is fixed at the latter value. The resulting fit is unacceptable, with  $\chi^2_{\nu} = 3.83$  for 1533 dof,  $kT = 0.40 \pm 0.01 \text{ keV}$ , and photon index  $\Gamma = 2.83 \pm 0.01$ . We show this fit in the lower panel of Figure 2. The large discrepancy between the column density value of the blackbody plus power-law analysis and that of Durant & van Kerkwijk (2006a) is likely to be due to the fact that the power-law component is artificial and, because of steep photon index values, needs to be attenuated significantly at low energies, requiring large  $N_{\text{H}}$  values.

We have also attempted to fit the combined X-ray spectra of 4U 0142+61 with two blackbodies and the hard X-ray power law. The resulting statistics ( $\chi^2_{\nu} = 1.19$  for 1532 dof) are acceptable, slightly better than blackbody plus power-law fits, but perform poorly compared to the physical STEMS model ( $\Delta\chi^2 = 354.8$ ,  $\Delta\nu = 2$ ). These fits do better than the blackbody plus power-law fits in obtaining  $N_{\text{H}}$  values ( $0.559 \pm 0.004 \times 10^{22} \text{ cm}^{-2}$ ) closer to those determined by Durant & van Kerkwijk (2006a). However, there are positive residuals that rise systematically above 5.0 keV, indicating that the two blackbody fits do

not capture the observed hardness of the 4U 0142+61 spectra fully, even with the contribution from the hard X-ray power-law component. For these fits, we obtain parameter values at  $kT_1 = 0.349 \pm 0.002$  and  $kT_2 = 0.719 \pm 0.003 \text{ keV}$ , consistent with those found by den Hartog et al. (2007).

#### 4. DISCUSSION

In this paper, we analyzed the archival *XMM-Newton* and *Chandra* data on 4U 0142+61 and showed that the X-ray spectrum of this magnetar can be fit very well with the surface thermal emission and magnetospheric scattering model. The model contains only four physical parameters, which can be tightly constrained from the spectral fits. The residuals are flat over the energy range of the observations, as shown in Figure 1, indicating the ability of our model to capture the shape of the continuum in the whole energy range.

Our model also allows us to determine the physical properties of the neutron star. We show in Figure 3 the confidence contours that we obtain for the surface magnetic field strength, temperature, the scattering optical, the particle velocity in the magnetosphere, and Galactic column density. We obtain tight constraints for these parameters. In particular, the narrow contours for the magnetic field strength and the temperature are because of the fact that they both cause small but detectable variations in the X-ray spectra, which, combined with high-quality spectra and a large number of data points, pin down the values of these parameters. The scattering optical depth contributes to both the hardness of the model spectra and to attenuating proton cyclotron features and is also well constrained by the observations.

The measured values of temperature, surface magnetic field strength, and magnetospheric parameters remain constant within statistical uncertainty for each data set because of the stability of the source over the observed period. Figure 3 also shows that for most parameters, the errors are uncorrelated.

Comparison of the STEMS model to data also gives us the chance to probe the magnetospheres of magnetars. The scattering optical depth of 3.57, we obtain in our analysis corresponds to a charged particle density in the magnetosphere that is approximately  $3 \times 10^5$  times higher than the Goldreich-Julian density for 4U 0142+61 (using the inferred dipole magnetic field strength and the spin period of the source). Note that the magnetospheric parameters that we report here differ from those given in the resonant cyclotron scattering model of Rea et al. (2007) both because that analysis fitted a different power-law index for the hard X-ray component and because it does not take into account the atmospheric effects but uses a canonical blackbody.

We have determined the surface magnetic field strength of 4U 0142+61 as  $4.75 \times 10^{14} \text{ G}$ . This value is quite close to the dipole field strength  $1.3 \times 10^{14} \text{ G}$  (Gavriil & Kaspi 2002), obtained from the spin-down rate of this source using the dipole spin-down formula, but is not in exact agreement as in the case of XTE J1810–197, where the two field strengths are equal (Güver et al. 2007). The small difference is likely due to the fact that our spectroscopic measurements are sensitive to the field strength at the surface of the neutron star, while the dipole spin-down method measures the magnetic field strength at the light cylinder. In addition, the dipole spin-down formula assumes a fiducial angle between the rotation and the magnetic axes that is not expected to be accurate on a source-by-source basis. Finally, recent (see, e.g., Spitkovsky 2006) numerical calculations on the structure of a rotating neutron star magnetosphere show violations of the vacuum assumption. Nevertheless, obtaining a surface field strength that is close to the dipole strength is a further

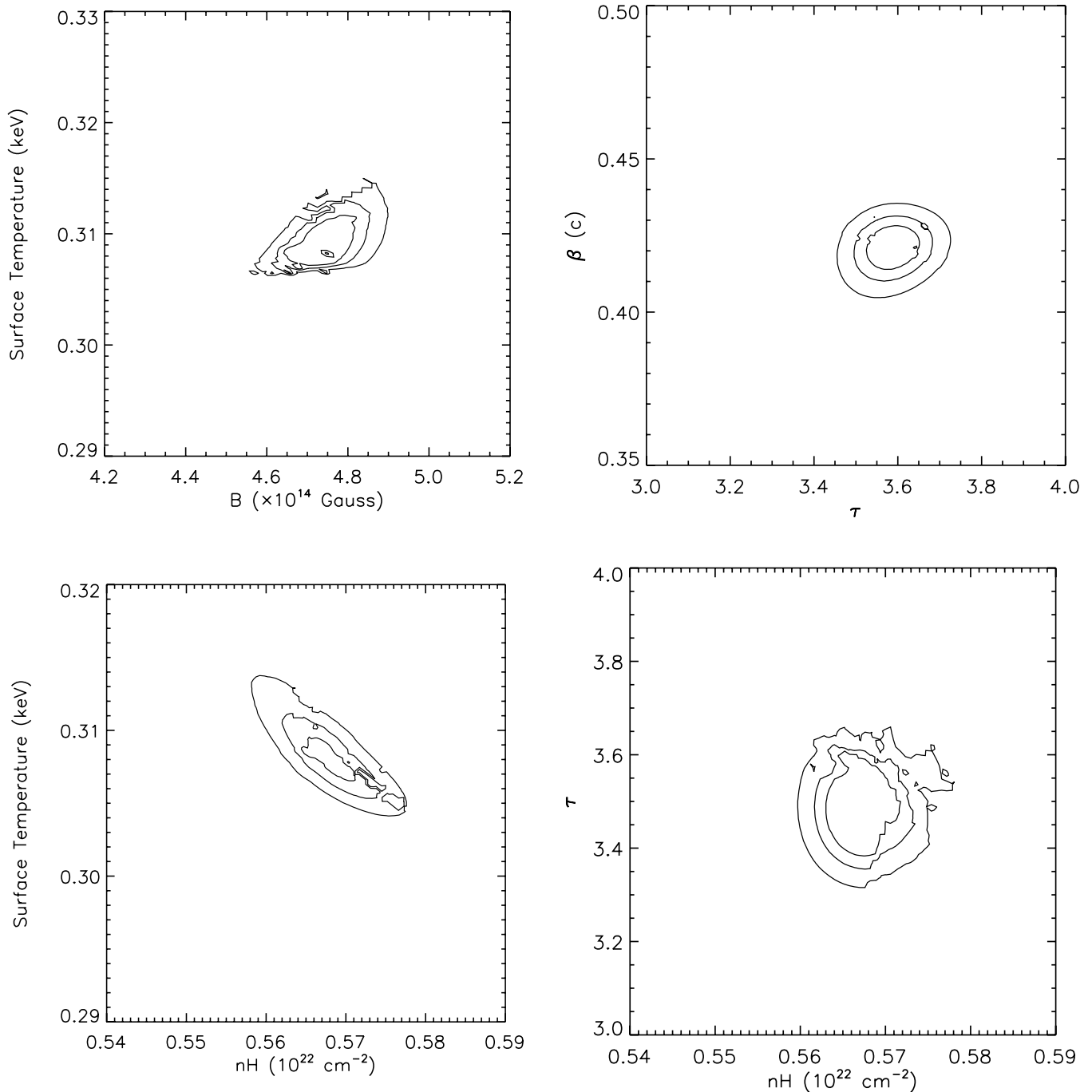


FIG. 3.—Confidence contour plots of different model parameters for the fits shown in Fig. 1. The three levels correspond to 1, 2, and 3  $\sigma$  confidence.

indication of the reliability of the measurements and the magnetar strength fields present in 4U 0142+61.

Finally, we calculate the area of the emitting region, assuming a gravitational redshift of 0.2 and a distance of 3.6 kpc (Durant & van Kerkwijk 2006b), and using the flux and the spectroscopically determined surface temperature. We obtain a radius of 10.8 km that does not vary between observations. Such a radius indicates that the emission arises from roughly three-quarters of the whole neutron star surface. This large surface area is suggestive: interestingly, the X-ray pulsed fraction (Woods & Thompson 2006) of 4U 0142+61 is 3.6%, which is the least among all the AXPs and SGRs.

We thank Keith Arnaud for his help during the creation of the XSPEC table model. This work makes use of observations obtained with *XMM-Newton*, an ESA science mission with instruments and contributions directly funded by ESA Member States and NASA. F. Ö. acknowledges support from NSF grant AST 07-08640 and from a Turkish Science and Technology Council Visiting Faculty fellowship. E.G. acknowledges partial support from the Turkish Academy of Sciences through grant E.G./TÜBA-GEBİP/2004-11. T. G. and E. G. acknowledge EU FP6 Transfer of Knowledge Project “Astrophysics of Neutron Stars” (MTKD-CT-2006-042722).

## REFERENCES

- Anders, E., & Grevesse, N. 1989, *Geochim. Cosmochim. Acta*, 53, 197
- Arnaud, K. A. 1996, in *ASP Conf. Ser. 101, Astronomical Data Analysis Software and Systems V*, ed. G. Jacoby & J. Barnes (San Francisco: ASP), 17
- den Hartog, P. R., Kuiper, L., Hermesen, W., Rea, N., Durant, M., Stappers, B., Kaspi, V. M., & Dib, R. 2007, *Ap&SS*, 308, 647
- den Hartog, R. H., et al. 2004, *ATel*, 293, 1
- Dib, R., Kaspi, V. M., Gavriil, F. P., & Woods, P. M. 2006, *ATel*, 845, 1
- . 2006b, *ApJ*, 650, 1070
- Gavriil, F. P., Dib, R., Kaspi, V. M., & Woods, P. M. 2007, *ATel*, 993, 1
- Gavriil, F. P., & Kaspi, V. M. 2002, *ApJ*, 567, 1067
- Gotthelf, E. V., & Halpern, J. P. 2007, *Ap&SS*, 308, 29
- Göhler, E., Wilms, J., & Staubert, R. 2005, *A&A*, 433, 1079
- Güver, T., Özel, F., Göğüş, E., & Kouveliotou, C. 2007, *ApJ*, 667, L73
- Güver, T., Özel, F., & Lyutikov, M. 2006, *ApJ*, submitted (astro-ph/0611405)
- Israel, G. L., Meregetti, S., & Stella, L. 1994, *ApJ*, 433, L25
- Juett, A. M., Marshall, H. L., Chakrabarty, D., & Schulz, N. S. 2002, *ApJ*, 568, L31
- Kaspi, V. M. 2007, *Ap&SS*, 308, 1
- Kaspi, V. M., Dib, R., & Gavriil, F. 2006, *ATel*, 794, 1
- Kaspi, V. M., Gavriil, F. P., Woods, P. M., Jensen, J. B., Roberts, M. S. E., & Chakrabarty, D. 2003, *ApJ*, 588, L93
- Kuiper, L., et al. 2006, *ApJ*, 645, 556
- Lai, D., & Ho, W. C. G. 2003, *ApJ*, 588, 962
- Lyutikov, M., & Gavriil, F. P. 2006, *MNRAS*, 368, 690
- Özel, F. 2001, *ApJ*, 563, 276
- . 2003, *ApJ*, 583, 402
- Özel, F., & Güver, T. 2007, *ApJ*, 659, L141
- Patel, S. K., et al. 2003, *ApJ*, 587, 367
- Rea, N., Turolla, R., Zane, S., Tramacere, A., Stella, L., Israel, G. L., & Campana, R. 2007, *ApJ*, 661, L65
- Spitkovsky, A. 2006, *ApJ*, 648, L51
- Thompson, C., & Duncan, R. C. 1996, *ApJ*, 473, 322
- Thompson, C., Lyutikov, M., & Kulkarni, S. R. 2002, *ApJ*, 574, 332
- White, N. E., Angelini, L., Ebisawa, K., Tanaka, Y., & Ghosh, P. 1996, *ApJ*, 463, L83
- Woods, P. M., & Thompson, C. 2006, in *Compact Stellar X-Ray Sources*, ed. W. Lewin & M. van der Klis (Cambridge: Cambridge Univ. Press), 547
- Woods, P. M., et al. 2005, *ApJ*, 629, 985